Journal of the Optical Society of Korea
Vol. 12, No. 1, March 2008, pp. 49-51

DOI: 10.3807/JOSK.2008.12.1.049

An Embedded Wide-Band Spiral Inductor for 10 Gb/s Optical Transceiver Applications

Young-Mi Kwon, Dong-Churl Kim, and Jong-In Shim*

Dept. of Electrical and Computer Engineering, Hanyang University, Ansan, 426-791, Korea

(Received March 6, 2008 : revised March 11, 2008)

The wide-band spiral inductor to be monolithically integrated on the AlN substrate as a choking inductor for a compact 10 Gb/s optical transmitter applications is investigated. In order to reduce the parasitic capacitance limiting the choking bandwidth, the AlN substrate is partially etched away, which is analyzed by using an equivalent circuit model. The measured S_{21} transmission response of the fabricated inductor is suppressed as low as -10 dB in the frequency range of 5 to 16 GHz.

OCIS codes : 250.0250, 250.3140

I. INTRODUCTION

As the demand for a 10 Gb/s transmission system increases, one of the most promising optical transceiver modules for the reduction of the cost as well as the size of the system is the 10 Gb/s small form factor pluggable (XFP) of the multi source agreement (MSA) [1], which requires a compact and uncooled transmitter optical sub-assembly (TOSA) operating at 85℃ without thermoelectric cooler up to 10 GHz [2]. In the design of a high-performance TOSA, the most crucial problem is the impedance matching from a driver IC to a laser chip. When the usual output impedance of the driver IC and the laser chip are 25 Ω and 5 Ω, respectively, it is proper to place a matching resistor of 20 Ω just in front of a laser chip on the signal line between the driver IC and the laser chip. In this case, however, when both the RF signal and the DC bias current are applied through the matching resistor, the DC bias current generates a large amount of Joule heat in the matching resistor, which in turn severely degrades the laser performance. Thus, it is preferable to decouple the RF line from the DC line. A spiral inductor makes it possible to not only separate the DC bias from the RF signal but also be monolithically embedded on sub-mount. For high-speed optoelectronic package, a high-performance inductor should be desired to have high self-resonant frequency (SRF) and a wide choking range. However, there have been no reports on high-frequency inductors dedicated to 10 Gb/s optical transmitter applications.

In this letter, a spiral inductor with a wide choking bandwidth is fabricated on the AlN substrate for the purpose of embedding on the 10 Gb/s TOSA sub-mount. The substrate is partially etched away in order to increase the choking bandwidth by reducing the parasitic capacitance. The equivalent electrical model of the inductor with considering the etching effect and high-frequency phenomena is also presented.

II. DESIGN AND FABRICATION

To be applied to the 10 Gb/s applications, the frequency characteristic of the spiral inductor is desired to block the frequency range of 0 to 15 GHz. However, since limited space on the TOSA sub-mount is available for the spiral inductor, it is very difficult to completely block the whole frequency range using only the integrated spiral inductor whose inductance is usually less than 10 nH. Then, we mounted a ferrite bead on the DC line outside TOSA which has a transmission of less than -10 dB in the frequency range of 0 to 5 GHz. Thus, the embedded spiral inductor should be designed such that the S_{21} transmission is less than -10 dB in the frequency range of 5 to 15 GHz.

We choose the AlN substrate as a TOSA sub-mount due to its good thermal conductivity and high-frequency characteristics. Fig. 1 shows a schematic structure of the fabricated spiral inductor. The structural parameters are selected as the metal line width (w) of 15 μm, the gap width (g) of 15 μm between the lines, and the turn numbers (N) of 5. The thin film technology is applied

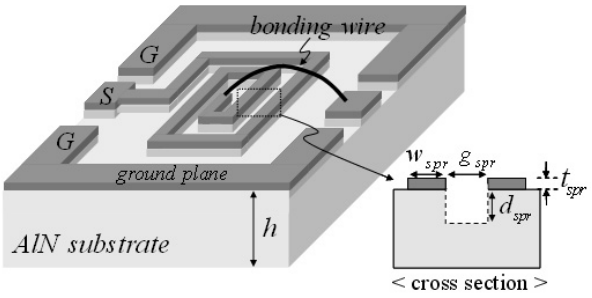

FIG. 1. Structure of a spiral inductor including a bonding wire and G-S-G probing pads.

to form the multilayered metallic structure of Ti (0.1 μm) / Pt (0.2 μm) / Au (4.7 μm). The G-S-G probing pads (130 μm × 100 μm) for the measurement and a bonding wire (300 μm-length and 25 μm-diameter) for electrical connection are presented.

The spiral inductor consists of the circuit elements of the inductance L, the parasitic capacitance C, and the parasitic resistance R. For design of the specified inductor, the high inductance, the high SRF and a moderate quality factor (Q-factor) are required. The most effective way to increase the inductance L is to introduce a narrow metal width w and a long metal length l, which in turn increases not only the coupling capacitance C between the metallic lines, but also the resistance R of line. There exist trade-offs among L, C, and R. Thus, it is necessary to reduce the C keeping with the L. We reduce C by etching the AlN substrate between the lines using the reactive ion etching (RIE) process. This is able to improve the SRF, Q-factor, and substrate loss between the lines [3].

III. CHARACTERIZATION AND RESULTS

We use the 2-Π model to capture the wide-band frequency characteristics above self-resonant frequency of the inductor [4]. The complete equivalent electrical model of the spiral inductor is shown in Fig. 2.

The inductance and the resistance of the inductor can be calculated by the following procedures. In single metal, since the dc current is uniformly distributed inside the conductor, it can be represented as a self inductance (L_0) and an ohmic resistance (R_0) in series. As the frequency goes up, the depth of current penetrating into the metal (skin depth) becomes smaller than the cross-sectional dimensions of the line, which decreases proportionally with the square root of frequency. To capture this skin effect, R_{skin} and L_{skin} are introduced in parallel to R_0. The magnetic field generated by neighboring lines changes the current distribution and results in a higher current density at the edges of the metal lines. This is described as the proximity effect and has a greater impact than the skin effect on the increase

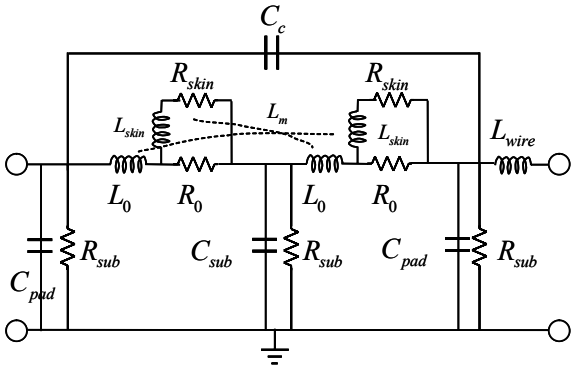

FIG. 2. The equivalent circuit model of the spiral inductor including skin effect, proximity effect, probing pads, and a bonding wire.

of resistance and degradation of Q-factor. This magnetic interaction between the external field and internal current is modeled by adding the mutual inductance (L_m) between L_0 and L_{skin}. The parameters of the linear circuit model are calculated by using the physical-based-closed form expressions which can explain the characterization of the range from DC to high frequency [4,5]. In this model, the original RL circuit is split into two parts.

The parasitic capacitances are considered in this model. They consist of the coupling capacitance (C_c) between adjacent lines and the substrate capacitance (C_{sub}) between the signal lines and the ground lines. To accurately quantify the C_c and the C_{sub} at high frequency, the distributed capacitance model was utilized [6]. Since our inductor has just co-planar ground planes without back metal, the C_c and the C_{sub} are changed and they are expressed as

$$C_c = \frac{1}{8}\sum_{k=1}^{n-1}\sum_{s=k+1}^{n} C_{k,s}\left(l_k + l_s\right)\left[p(s)-p(k)\right]^2 + \frac{1}{8}\sum_{k=1}^{n} C_{k,n+1}\left(l_k + l_{n+1}\right)\left[1-p(k-1)-p(k)+p(n)\right]^2 \quad (1)$$

$$C_{sub} = \frac{1}{8}\sum_{k=1}^{n} C_{k,sub} l_k \left[2-p(k-1)-p(k)\right]^2 + \frac{1}{2}\sum_{k=1}^{n} C'_{k,sub} w\left[2-p(k-1)-p(k)\right]^2 \quad (2)$$

where $C_{k,s}$ is a coupling capacitance between kth and sth lines per unit length, $C_{k,sub}$ is a substrate capacitance of kth line per unit length, l_k is the total length of kth turn, and $p(k)$ is the effective length of kth turn. The values of $C_{k,s}$ and $C_{k,sub}$ can be obtained by using 2-D structural parameter extractor. The parasitic capacitances according to etching depth (d) are calculated and shown in Fig. 3 where C_{pad} indicates the capacitance due to the probing pads. For the substrate of $d = 2.5$ μm, the capacitances are reduced by approximately 15% compared to those of the substrate without etching.

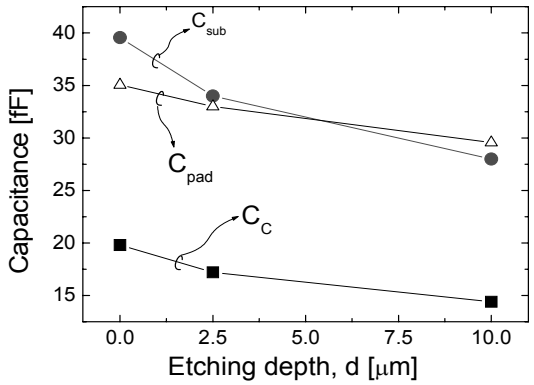

FIG. 3. Calculated capacitances according to the etching depth d of the spiral inductor.

TABLE 1. Calculated Electrical Parameters of Spiral Inductor with and without Etched Substrates.

Parameters	No etching	2.5 μm-etch
C_c	20 fF	**18** fF
C_{sub}	40 fF	**34** fF
C_{pad}	35 fF	**33** fF
L_0	4.6 nH	4.6 nH
L_{skin}	8.65 nH	8.65 nH
L_m	0.26 nH	0.26 nH
R_0	1.6 Ω	1.6 Ω
R_{skin}	2.4 Ω	2.4 Ω
R_{sub}	9 kΩ	9 kΩ
L_{wire}	0.2 nH	0.2 nH

The extracted parameters of the spiral inductor are listed in Table 1 where L_{wire} is the bonding wire inductance. The measured S_{21} response for $d = 2.5$ μm is shown in Fig. 4 by the dotted circles. The calculated S_{21} responses of the equivalent circuit are also plotted with solid lines for two different substrate etching conditions of $d = 0$ and 2.5 μm. The measured frequency response shows good agreement with the simulated one. We obtained very good blocking characteristics of less than -10 dB in the frequency range from 5 to 16 GHz, Q-factor of 20, and SRF of 6.5 GHz. It can be clearly seen that the substrate etching in spiral inductors is very simple and effective method to suppress the high-frequency component coupling in the DC bias line which can increase the transient chirp of the driving laser. There exist some differences in the measured and simulated S_{21} responses. The difference in the resonance frequency around 12-13 GHz may be produced by fabrication errors from the designed capacitor structure. The deviation around 18-20 GHz frequency range may result from the limitations of the lumped model shown in Fig. 2 where higher order resonance modes are not considered.

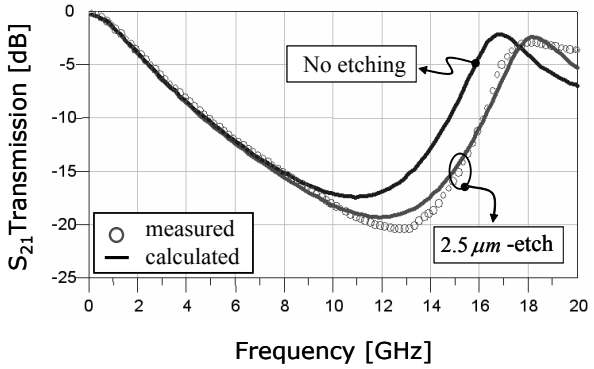

FIG. 4. Measured and calculated S_{21} parameters of spiral inductor with and without substrate etching ($w = 15$ μm, $g = 15$ μm, $N = 5$, and $t = 5$ μm).

IV. CONCLUSIONS

The wide-band spiral inductor for high-speed opto-electronic package focused especially on the applications of compact 10 Gb/s optical transmitter for XFP module has been designed and fabricated. By etching the substrate of the spiral inductor as 2.5 μm, the parasitic capacitance is reduced approximately by 15% and the measured and the calculated S_{21} transmission is suppressed as low as -10 dB in the frequency range of 5 to 16 GHz.

*Corresponding author: jishim@giga.hanyang.ac.kr

REFERENCES

[1] XFP MSA Group, http://www.xfpmsa.org.
[2] Y. Keh, M. Park, Y. Kim, D. Kim, and D. Jang, "A novel 10 Gbps TO laser package," *in Proc. European Conference on Optical Communication*, pp. 84-85, 2003.
[3] L.-H. Lu, G. E. Ponchak, P. Bhattacharya, L. P. B. Katehi, "High-Q X-band and K-band micromachined spiral inductors for use in Si-based integrated circuits," *in Dig. IEEE MTT-S Topical Meeting on Silicon Monolithic Integrated Circuits in RF Systems*, pp. 108-112, 2000.
[4] Y. Cao, R. A. Groves, X. Huang, N. D. Zamdmer, J.-O Plouchart, R. A. Wachnik, T.-J. King, and C. Hu, "Frequency-independent equivalent-circuit model for on-chip spiral inductors," *IEEE J. Solid-State Circuits*, Vol. 38, No. 3, pp. 419-426, 2003.
[5] H. M. Greenhouse, "Design of planar rectangular microelectronic inductors," *IEEE Trans. on Parts, Hybrids, Packaging*, Vol. 10, No. 2, pp. 101-109, 1974.
[6] C. Wu, C. C. Tang, and S. I. Liu, "Analysis of on-chip spiral inductors using the distributed capacitance model," *IEEE J. Solid-State Circuits*, Vol. 38, No. 6, pp. 1040-1044, 2003.